PHYSICAL REVIEW D **94,** 055020 (2016)

First results on bilepton production based on LHC collision data and predictions for run II

A. A. Nepomuceno* and F. L. Eccard

Departamento de Ciências da Natureza, Universidade Federal Fluminense, Rua Recife, 28890-000 Rio das Ostras, Rio de Janeiro, Brazil

B. Meirose†

Department of Physics, University of Texas at Dallas, 800 West Campbell Road, Richardson, Texas 75080-3021, USA

(Received 16 May 2016; published 16 September 2016)

The LHC potential for discovering doubly charged vector bileptons is investigated considering the measurable process $pp \to \mu^+\mu^+\mu^-\mu^- X$. The study is performed assuming different bilepton and leptoquark masses. The process cross section is calculated at leading order using the CALCHEP package. Combining the calculation with the latest ATLAS experiment results at a center-of-mass energy of 7 TeV, bounds on bilepton masses based on LHC data are derived for the first time. The results exclude bilepton masses in the range of 250 GeV to 500 GeV at 95% C.L., depending on the leptoquark mass. Moreover, minimal LHC integrated luminosities needed for discovering and for setting limits on bilepton masses are obtained for 13 TeV center-of-mass energy. Simulated events are passed through a fast parametric detector simulation using the DELPHES package.

DOI: 10.1103/PhysRevD.94.055020

I. INTRODUCTION

The first run of the LHC has discarded or disfavored several new physics scenarios, with no significant excess of events compared to the Standard Model (SM) expectations having yet been observed by any of the LHC experiments in a plethora of different final states. The most significant result, the discovery of a particle consistent with the SM Higgs boson [1,2], while outstanding, has so far only strengthened our confidence in the SM. However, the famous SM puzzles that have motivated the pre-LHC model building era are still unsolved and very much alive, desperately needing guidance from experiment to be unraveled.

One of the dramatic effects caused by the LHC results is that, while some beyond SM (BSM) searches became less appealing, others may now experience renewed interest from the particle physics community. A good example is the search for the so-called bileptons.

Bileptons are bosons with two units of leptonic number [3]. They couple to two leptons, but not to two SM quarks. Bileptons do however couple to leptoquarks, which carry both baryon and lepton numbers. Scalar bileptons are predicted by theories with an enlarged Higgs sector (such as left-right models) as well as by models that generate neutrino Majorana masses. Nongauge vector bileptons are present in composite theories, while heavy gauge vector bileptons, the ones studied in this article, are present when the SM is embedded in a larger gauge group. The most important and natural class of models where vector bileptons appear are the 331 models [4–7], and all calculations in this article are based on them. Our main results should however hold for other models containing vector bileptons.

A. Objective, motivations, and paper organization

The objective of the present article is to study doubly charged vector bilepton production in the channel $p, p \to \mu^+\mu^+\mu^-\mu^- X$. The main motivation is to obtain experimental limits on bileptons based on LHC collision data. To do this, public data plots from the ATLAS Collaboration are used and reinterpreted for the same channel [8]. The current article provides therefore the first, and to this date, only existing experimental limits for vector bileptons using LHC data. Furthermore, a fast detector simulation for bilepton signatures is performed and used to estimate the five-sigma bilepton discovery potential for the LHC's run II at 13 TeV center-of-mass energy. These results complement our previous work where we provided a theoretical estimation of the reach of the process $p, p \to e^\mp e^\mp \mu^\pm \mu^\pm X$ to discover or exclude vector bileptons at 14 TeV [9].

The paper is organized as follows. In Sec. II a brief review of the 331 models is given, with a focus on the features that are most relevant to the current analysis. In Sec. III, a brief discussion on bilepton experimental limits in light of the LHC's run I results is presented. Section IV describes the Monte Carlo (MC) and detector simulation

*andrenepomuceno@id.uff.br
†Bernhard.Meirose@cern.ch

procedures. In Sec. V the 95% C.L. experimental limits based on 7 TeV LHC collision data are presented. The doubly charged vector bilepton discovery potential for the four-muons channel at 13 TeV is shown in Sec. VI. Conclusions are presented in Sec. VII.

II. 331 MODELS

The 331 models are based on the gauge symmetry $SU(3)_C \otimes SU(3)_L \otimes U(1)_X$, hence their name. They can generically be classified according to how they cancel chiral anomalies. For example, there are anomaly-free 331 models requiring only one family of quarks and leptons, although the majority of the models studied in the literature are three-family models [10]. We are interested in particular versions of the three-family models that predict a new neutral gauge boson Z' and four vector bileptons $Y^{\pm}$ and $Y^{\pm\pm}$ in the gauge sector. In addition, the fermion sector of the class of 331 models studied in the present article contains three new heavy leptoquarks: T_1, with electric charge $\pm 5/3$, and D_1 and D_2, both with $\pm 4/3$ of electric charge. The production and decay of the 331 leptoquarks at the LHC have been investigated in Ref. [11].

There are several reasons why three-family 331 models are good candidates to describe nature at the TeV scale and we refer the reader to Ref. [9] for a review. One of their most striking motivations is that they offer an elegant solution for SM's family replication problem. This is achieved through two main ingredients. The first is that the cancellation of triangle anomalies is nontrivial, taking place between families, which can only happen if the number of families is a multiple of three. The second ingredient is QCD's asymptotic freedom, which requires the number of quark generations to be less than five. These two conditions imply that the number of families must be exactly three.

Both the exotic leptoquarks and the new gauge bosons acquire mass through spontaneous symmetry breaking (SSB) of the $SU(3)_L \otimes U(1)_X$ gauge sector. There are distinct ways how this can be accomplished and the different possibilities of Higgs sectors define further 331 model subversions within the three-family 331 models. The 331 minimal model is a particular example of one of these subversions that uses the minimal Higgs structure for SSB. The model continues to attract attention because it requires the bilepton and Z' masses to be bound in a similar way as the W and Z masses are bound in the SM. However, other than the theoretical aesthetic appeal it provides through this SM resemblance, there is no real compelling reason, neither phenomenological nor experimental, to give the minimal model any privileged treatment. Indeed, there is already circumstantial evidence that, to some degree, disfavors this particular version experimentally, even though it has not yet been fully excluded [9].

III. BILEPTONS BEFORE AND AFTER LHC RUN I

Even before LHC's first run, limits on vector bileptons suggested that observing those particles during run I was a rather unfavorable scenario. The reason is as follows. The two most useful mass limits for vector bileptons are $M_Y > 740$ GeV [12], a limit derived from experimental limits on fermion pair production at LEP and lepton-flavor charged lepton decays, and $M_Y > 850$ GeV [13,14], a limit established from muonium-antimuonium conversion. In Ref. [9], we have predicted that the 5σ discovery potential for LHC's run I at 7 TeV center-of-mass energy, using 10 fb^{-1} of integrated luminosity, was only around 540 GeV. Even the full 20 fb^{-1} of data collected in run I at 8 TeV center-of-mass energy would not have been enough to surpass those two limits. However, both limits are not general, and consequently, a discovery could not have been completely discarded. The first limit has been obtained with LEP data, and as such, it is restricted to the leptonic mixing matrix being diagonal, since in 331 models, the leptons mix by a Cabibbo-Kobayashi-Maskawa-like mixing matrix whose elements have not been measured. The second limit is even more restrictive and depends on the assumption that the bilepton couplings are flavor diagonal. Vector bilepton experimental limits making use of hadronic beams are therefore obtained in this paper for the first time. LHC constraints on general doubly charged scalars, not necessarily scalar bileptons, were studied in Ref. [15].

The situation for the LHC's run II is quite different. Not only will the LHC be able to probe the already searched region by LEP in a more general way using hadronic beams, it will also probe a completely new bilepton mass region around 1 TeV.

IV. MONTE CARLO AND DETECTOR SIMULATIONS

The 331 model is implemented in the CALCHEP event generator [16] following Refs. [17–19] for bilepton trilinear gauge interactions, Z' couplings to fermions, and bilepton interactions with leptons, respectively. Bilepton interactions with 331 model leptoquarks are also taken into account [9]. The implementation is validated and extensively tested for consistency and unitarity.

CALCHEP is used to calculate cross sections and to produce events for several bilepton mass points for bilepton pair production. The generated events are processed by PYTHIA 8 [20,21] for hadronization and decays. A fast detector simulation is performed using DELPHES [22]. The DELPHES package is provided with different configurations to simulate the ATLAS or CMS responses. In this work, the Snowmass Combined LHC Detector configuration is used, which is a general detector simulation combining ATLAS and CMS features [23]. The leptoquark masses are assumed to be between 100 GeV and 800 GeV, and the Z' mass to be

3 TeV. This Z' mass value is chosen so that it is slightly above the current experimental limits [24]. For bileptons, the mass range considered is 200 GeV to 1000 GeV in steps of 100 GeV. The CTEQ6L1 [25] parton distribution function (PDF) set is used in the calculations.

In the process $p, p \to Y^{++}Y^{--} \to \mu^+\mu^+\mu^-\mu^- X$, the bilepton pair is produced through a Drell-Yan process intermediated by the photon and the Z^0 and Z' bosons. The on-shell Z' exchange gives a large contribution for $M_{Z'} < 1$ TeV [18]. Thus, for the $M_{Z'}$ value that we are considering (3 TeV), the bilepton pair is produced mainly via γ and Z^0 exchange, although including the Z' contribution is still needed to guarantee unitary.

Bileptons are also produced via a t-channel with a leptoquark exchange for the subprocesses $u\bar{u} \to Y^{++}Y^{--}$, $c\bar{c} \to Y^{++}Y^{--}$, and $b\bar{b} \to Y^{++}Y^{--}$. These additional channels are needed in order to guarantee that all relevant quark subprocesses respect unitarity. The Feynman diagrams for the processes are shown in Fig. 1.

It worth mentioning that, since the 331 models foresee additional scalars, they may increase the Z' width. However, the Z' partial width to scalars has no significant effect on the bilepton pair production cross section, and therefore these extra channels do not contribute to our analysis.

V. LHC RUN I: 7 TEV BILEPTON EXPERIMENTAL LIMITS

The ATLAS Collaboration has set upper limits on the cross section for the doubly charged Higgs production in different final states at 7 TeV [8]. The data sample corresponds to an integrated luminosity of 4.7 fb^{-1}. The 95% C.L. observed limits were placed as a function of the hypothesized boson mass, as shown in Fig. 2. These ATLAS limits were obtained for the number of lepton pairs originating from $H^{\pm\pm}$ in different mass windows. They are converted to limits on the cross section times branching ratio using the acceptance times of efficiency derived from MC simulation. The ATLAS expected limits are the median values resulting from a large number of simulated pseudoexperiments, assuming that no signal is present. Since bileptons are narrow resonances like the doubly charged Higgs (and therefore, they have similar acceptances and efficiencies), the ATLAS results can be used to derive limits on the bileptons' masses.

The theoretical cross section times branching ratio for the process $p, p \to \mu^+\mu^+\mu^-\mu^- X$, considering different bilepton and leptoquark masses, is calculated and compared with the cross-section limits obtained by ATLAS. The bilepton upper cross-section limit is derived from the intersection between the theoretical and the experimental curves. This limit is translated in the lower limit on the bilepton mass. Figure 2 illustrates the procedure for three different leptoquark masses. For $M_Q = 100$ GeV, vector bileptons with masses below 250 GeV are excluded. The strongest limit that can be derived for bileptons with 7 TeV data is $M_Y > 520$ GeV, corresponding to a leptoquark mass of $M_Q = 600$ GeV. Figure 3 shows the exclusion region on the $M_Y \times M_Q$ plane, obtained from Fig. 2, considering six values of leptoquark mass between 100 GeV and 600 GeV. The blue (dark) region is excluded at 95% C.L. These results agree very well with our prediction for bilepton exclusion with 5 fb^{-1} of data at 7 TeV (see Table II of Ref. [9]). Bileptons with masses between 250 GeV and 520 GeV, depending on the leptoquark mass, are excluded.

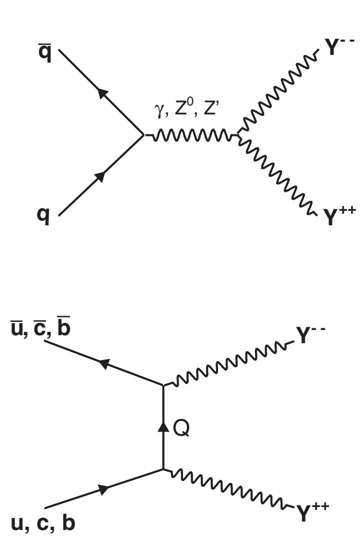

FIG. 1. Feynman diagrams contributing to bilepton pair production at the LHC.

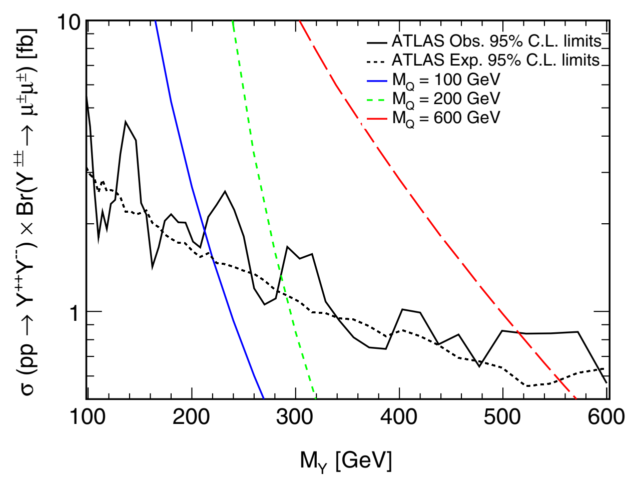

FIG. 2. Upper limits on $\sigma \times Br$. The black solid and dashed lines represent the ATLAS observed and expected limits, respectively. The blue, green, and red lines are the cross section times branching ratio for bilepton production decaying into muons for different values of the leptoquark mass.

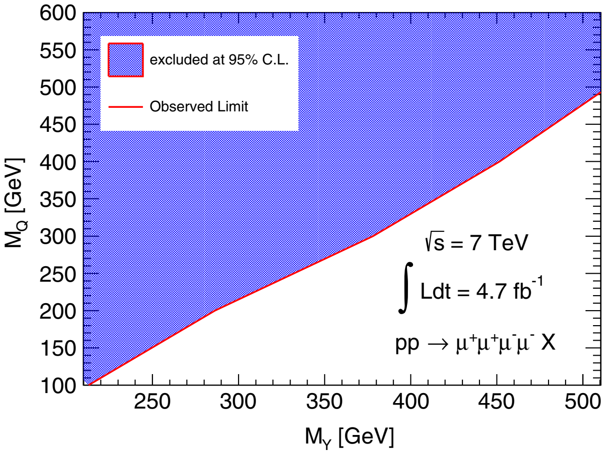

FIG. 3. Exclusion region on the $M_Y \times M_Q$ plane.

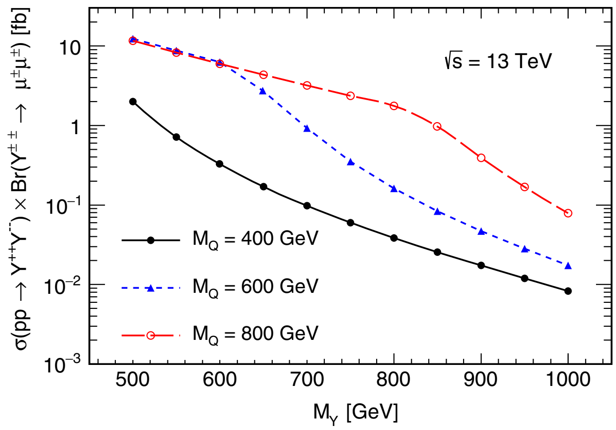

FIG. 5. Cross section for bilepton production at 13 TeV.

VI. LHC RUN II: 13 TEV BILEPTON THEORETICAL REACH

The LHC potential for discovering vector bileptons at a center-of-mass energy of 13 TeV is studied. Figures 4 and 5 show the bilepton width and cross section for doubly charged bilepton production and subsequent decay to muons at 13 TeV for three different leptoquark masses. The values of bilepton and leptoquark masses were chosen in a region beyond the region excluded. Bileptons decaying into leptoquarks explains the cross-section behavior observed for $M_Q = 600$ GeV and $M_Q = 800$ GeV. For $M_Y > M_Q$, bilepton decays like $Y^{\pm\pm} \to qQ$ become kinematically allowed, which causes $Br(Y^{\pm\pm} \to \ell^{\pm}\ell^{\pm})$ to decrease.

A fast detector simulation using DELPHES is performed to estimate the acceptance and efficiency for reconstructing bileptons. In the analysis of the reconstructed events, at least four muons are initially selected. As each bilepton decays to a pair of same-sign muons, there are four muons in the final state, two negatively and two positively charged. If more than four muons are found, the ones with higher transverse momentum (p_T) are chosen. All muons must be inside the detector acceptance ($|\eta| < 2.5$) and have $p_T > 20$ GeV. The product of the acceptance and the selection efficiency after these cuts is around 80%. As there is no trigger efficiency included in the simulation, we multiply the reconstruction efficiency by the expected trigger efficiency of 80% [26]. The overall efficiency is then 64%. The dominant background in this search is processes that can produce four muons in the final state. We have considered Higgs and ZZ productions, both decaying to four muons. The Higgs background is found negligible above the muons' invariant mass of 500 GeV. Figures 6 and 7 show the invariant mass distributions for each same-sign muon pair. The yellow histogram is the background, and the open histograms represent two possible bilepton signals. As the bileptons are produced in pairs, each same-sign muon pair has the same invariant mass distribution.

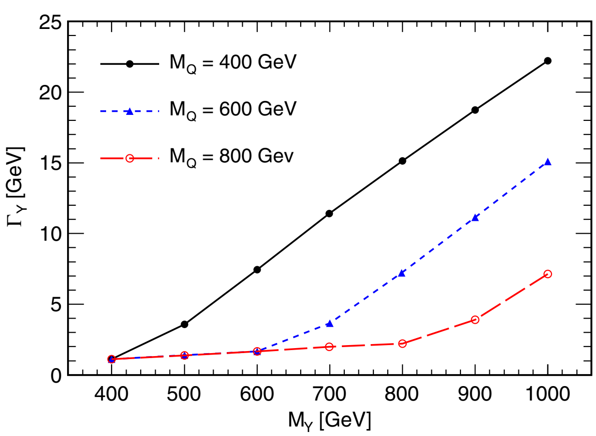

FIG. 4. Bilepton width as a function of bilepton mass for three different leptoquark masses.

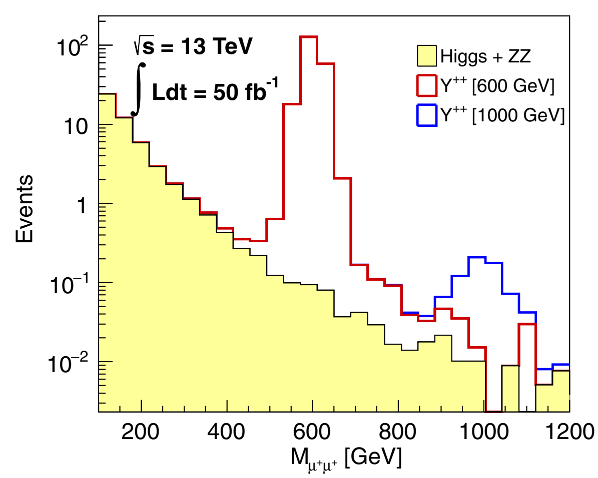

FIG. 6. Invariant mass distributions for same-sign muon pairs produced by the background and by bilepton decay, assuming an integrated luminosity of 50 fb^{-1}. The open red/blue histograms are two possible positively charged bilepton signals.

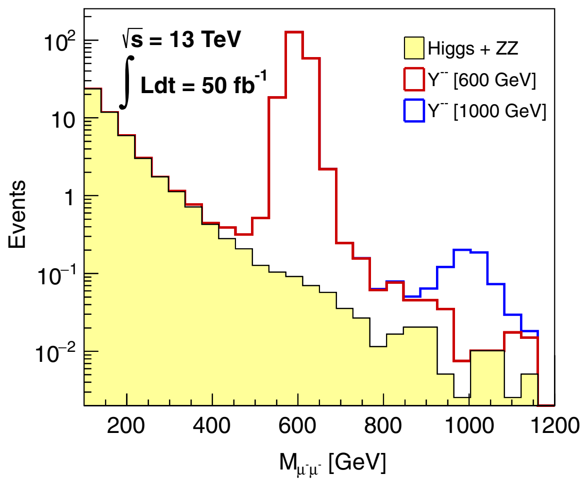

FIG. 7. Same as Fig. 6, but for negatively charged bileptons.

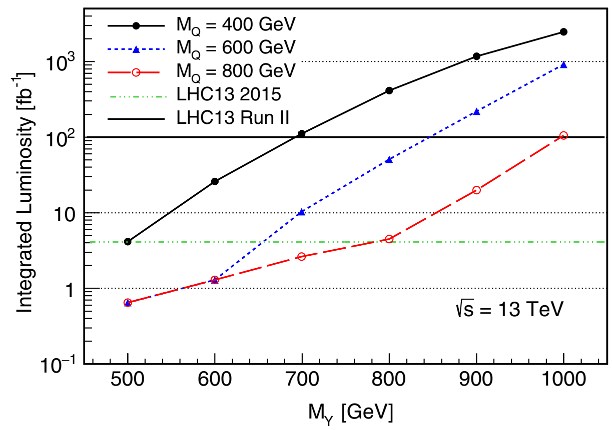

FIG. 8. Minimal integrated luminosity needed for a 5σ discovery of doubly charged vector bileptons in the four-muon final state.

The minimal integrated luminosity needed to discover a doubly charged vector bilepton in the four-muon channel at LHC is calculated by comparing the background and signal invariant mass distributions through a chi-square analysis. The test is performed within a dimuon mass window of $[M_Y - 5\Gamma_{\rm rec}, M_Y + 5\Gamma_{\rm rec}]$, where $\Gamma_{\rm rec}$ is the width of a Gaussian fitted to the signal invariant mass distribution of the muon pairs. The bin width of the distribution is chosen so that it is larger than the invariant mass resolution determined from the detector simulation. For each value of bilepton and leptoquark mass, a hypothesis test is performed using as test statistic a chi-square given by [27]

$$\chi^2 = \sum_{i=1}^{n} \left[2(N_i - \nu_i) + 2(\nu_i + 1)\log\left(\frac{2\nu_i + 1}{2N_i + 1}\right)\right] \qquad (1)$$

where n is the number of bins; ν_i is the background mean value, in the ith bin, determined from a large simulated sample; and N_i is the number of events in each bin of the tested histogram. By conducting this analysis for 5000 MC pseudoexperiments, we can determine the chi-square distributions of the background-only and background-plus-signal hypotheses. The significance level (P-value) is obtained by integrating the tail of the χ^2 distribution of the background-only hypothesis

$$P = \int_{\langle\chi_s^2\rangle}^{\infty} f(z)dz \qquad (2)$$

where $\langle\chi_s^2\rangle$ is the χ^2 most probable value for the background-plus-signal hypothesis. In order to estimate the amount of data needed to claim a bilepton discovery, the integrated luminosity is increased until we have $P < 3.0 \times 10^{-7}$, which corresponds to a significance of 5σ. The results are shown in Fig. 8.

The horizontal dashed-dotted line in Fig. 8 represents the integrated luminosity delivered by the LHC in the first phase of the 13 TeV run ($\sim$4 fb^{-1}). Bileptons with masses up to 800 GeV can be probed with the available data. By the end of run II, with an integrated luminosity of 100 fb^{-1}, bileptons with masses between 500 GeV and 1000 GeV could be discovered.

If no bilepton signal is found in run II, the new LHC data can considerably extend the current limits of these particles. In order to calculate the exclusion limits that can be reached with a given integrated luminosity, a single bin analysis applying a Bayesian technique is done. An implementation of the method is available in the MCLIMIT program [28,29]. This approach assumes that the signal adds incoherently to the background. The inputs for the calculations are the expected number of signal and background events obtained from the detector simulation. Figure 9 shows the expected limits on $\sigma \times Br$, assuming 50 fb^{-1} of data, for different bilepton mass hypotheses. The black dashed line is the median values of the limits obtained from 1000 pseudoexperiments, and the yellow and green bands

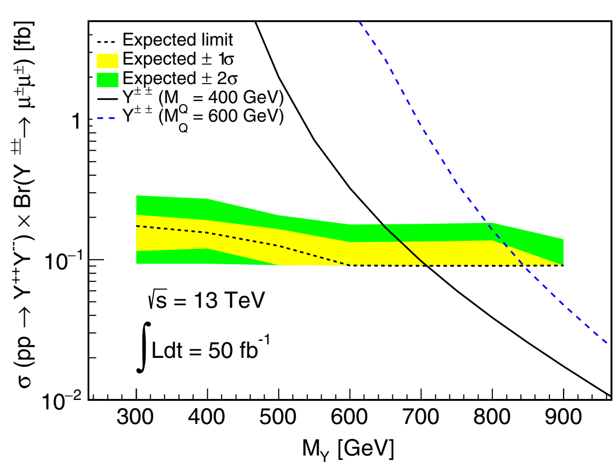

FIG. 9. Upper limits on $\sigma \times Br$, assuming 50 fb^{-1} of data at 13 TeV.

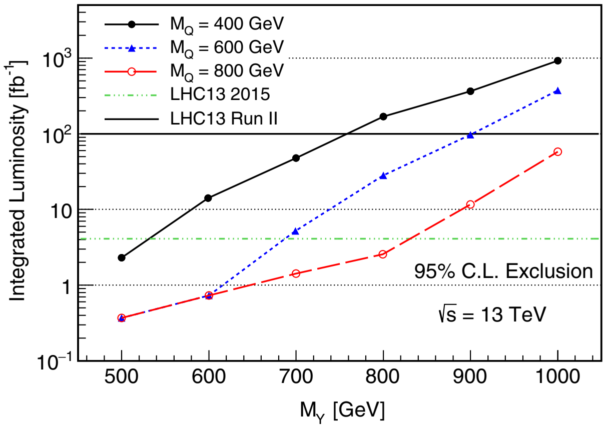

FIG. 10. Minimal integrated luminosity needed to exclude bileptons of a given mass, for three different leptoquark masses.

represent the 1σ and 2σ variation around the median, respectively. The lower bound $M_Y > 850$ GeV can be reached with this luminosity. This procedure is repeated for different values of the integrated luminosity, and for each of them, a lower mass limit for bileptons/leptoquarks is obtained. The results are shown in Fig. 10. With 100 fb^{-1} of data, the bilepton limits can be extended above 1000 GeV in the most optimistic scenario. With 300 fb^{-1}, the integrated luminosity expected for the LHC's run III, masses up to 900 GeV can be excluded for the lowest branching ratio considered. In any case, one will still be below the theoretical upper limit $M_Y < 4$ TeV imposed by the 331 model [30].

It is interesting to point out the interplay between the masses of bileptons and of the leptoquarks in the 331 model and that excluding one mass or the other depends intrinsically on both mass choices. For instance, if bileptons are as massive as 1 TeV, a leptoquark mass of 400 GeV is still allowed in run III as far as the process $p, p \to \mu^+\mu^+\mu^-\mu^-X$ is concerned.

VII. CONCLUSIONS

Exclusion limits on bilepton masses based on LHC real-data results at 7 TeV center-of-mass energy are derived. Bilepton masses in the range $250 < M_Y < 520$ GeV are excluded at 95% C.L. The LHC potential to observe doubly charged vector bileptons at 13 TeV center-of-mass energy in pp collisions is also investigated. Taking into account reconstruction and trigger efficiencies of muon detection, bilepton masses between 500 GeV and 1000 GeV can be observed by the end of run II. With the available data at 13 TeV, lower bounds from 530 GeV to 830 GeV can be estimated for the bilepton mass. New data from run II can push the current limits up to 1040 GeV. Considering the theoretical constraint imposed by the 331 models on bilepton mass, our results show that the model cannot be fully excluded even in run III.

ACKNOWLEDGMENTS

B. Meirose's work has been supported by U.S. DOE Grant No. DE-SC0010384. A. Nepomuceno thanks CNPq for the financial support.

[1] G. Aad *et al.* (ATLAS Collaboration), Phys. Lett. B **716**, 1 (2012).
[2] S. Chatrchyan *et al.* (CMS Collaboration), Phys. Lett. B **716**, 30 (2012).
[3] F. Cuypers and S. Davidson, Eur. Phys. J. C **2**, 503 (1998).
[4] P. H. Frampton, Phys. Rev. Lett. **69**, 2889 (1992).
[5] F. Pisano and V. Pleitez, Phys. Rev. D **46**, 410 (1992).
[6] D. Ng, Phys. Rev. D **49**, 4805 (1994).
[7] A. G. Dias, J. C. Montero, and V. Pleitez, Phys. Lett. B **637**, 85 (2006).
[8] G. Aad *et al.* (ATLAS Collaboration), Eur. Phys. J. C **72**, 2244 (2012).
[9] B. Meirose and A. A. Nepomuceno, Phys. Rev. D **84**, 055002 (2011).
[10] W. A. Ponce, J. B. Florez, and L. A. Sanchez, Int. J. Mod. Phys. A **17**, 643 (2002).
[11] A. Alves, E. R. Barreto, and A. G. Dias, Phys. Rev. D **86**, 055025 (2012).
[12] M. B. Tully and G. C. Joshi, Phys. Lett. B **466**, 333 (1999).
[13] L. Willmann *et al.*, Phys. Rev. Lett. **82**, 49 (1999).
[14] V. Pleitez, Phys. Rev. D **61**, 057903 (2000).
[15] F. del guila and M. Chala, J. High Energy Phys. 03 (2014) 027.
[16] A. Belyaev, N. D. Christensen, and A. Pukhov, Comput. Phys. Commun. **184**, 1729 (2013).
[17] H. N. Long and D. V. Soa, Nucl. Phys. **B601**, 361 (2001).
[18] B. Dion, T. Gregoire, D. London, L. Marleau, and H. Nadeau, Phys. Rev. D **59**, 075006 (1999).
[19] P. H. Frampton and D. Ng, Phys. Rev. D **45**, 4240 (1992).
[20] T. Sjostrand, S. Mrenna, and P. Z. Skands, J. High Energy Phys. 05 (2006) 026.
[21] T. Sjostrand, S. Mrenna, and P. Z. Skands, Comput. Phys. Commun. **178**, 852 (2008).
[22] J. de Favereau, C. Delaere, P. Demin, A. Giammanco, V. Lematre, A. Mertens, and M. Selvaggi (DELPHES 3 Collaboration), J. High Energy Phys. 02 (2014) 057.
[23] J. Anderson *et al.*, arXiv:1309.1057.
[24] C. Salazar, R. H. Benavides, W. A. Ponce, and E. Rojas, J. High Energy Phys. 07 (2015) 096.

[25] J. Pumplin, D. R. Stump, J. Huston, H.-L. Lai, P. Nadolsky, and W.-K. Tung, J. High Energy Phys. 07 (2002) 012.
[26] The ATLAS collaboration, Report No. ATLAS-CONF-2011-021, 2011.
[27] F. M. L. Almeida, Jr., M. Barbi, and M. A. B. do Vale, Nucl. Instrum. Methods Phys. Res., Sect. A **449**, 383 (2000).
[28] T. Junk, CDF8128, 2007.
[29] J. Heinrich, CDF7587, 2005.
[30] P. H. Frampton, Phys. Lett. B **747**, 187 (2015).